Macromolecules

Article

pubs.acs.org/Macromolecules

Reversibly Manipulating the Surface Chemistry of Polymeric Nanostructures via a "Grafting To" Approach Mediated by Nucleobase Interactions

Zan Hua,[†] Robert Keogh,[†] Zhen Li,[‡] Thomas R. Wilks,[†] Guosong Chen,[‡] and Rachel K. O'Reilly*[,†]

[†]Department of Chemistry, University of Warwick, Gibbet Hill Road, Coventry CV4 7AL, U.K.

[‡]The State Key Laboratory of Molecular Engineering of Polymers and Department of Macromolecular Science, Fudan University, Shanghai 200433, China

Supporting Information

ABSTRACT: "Grafting to" polymeric nanostructures or surfaces is a simple and versatile approach to achieve functionalization. Herein, we describe the formation of mixed polymer-grafted nanoparticles through a supramolecular "grafting to" method that exploits multiple hydrogen-bonding interactions between the thymine (T)-containing cores of preformed micelles and the complementary nucleobase adenine (A) of added diblock copolymers. To demonstrate this new "grafting to" approach, mixed-corona polymeric nanoparticles with different sizes were prepared by the addition of a series of complementary diblock copolymers containing thermoresponsive poly(*N*-isopropylacrylamide) (PNIPAM) to a preformed micelle with a different coronal forming block, poly(4-acryloylmorpholine) (PNAM). PNIPAM chains were distributed throughout the corona and facilitated a fast and fully reversible size change of the resulting mixed-corona micelles upon heating. Through the introduction of an environmentally sensitive fluorophore, the reversible changes in nanoparticle size and coronal composition could be easily probed. Furthermore, preparation of mixed-corona micelles also enabled ligands, such as D-mannose, to be concealed and displayed on the micelle surface. This supramolecular "grafting to" approach provides a straightforward route to fabricate highly functionalized mixed polymeric nanostructures or surfaces with potential applications in targeted diagnosis or therapy and responsive surfaces.

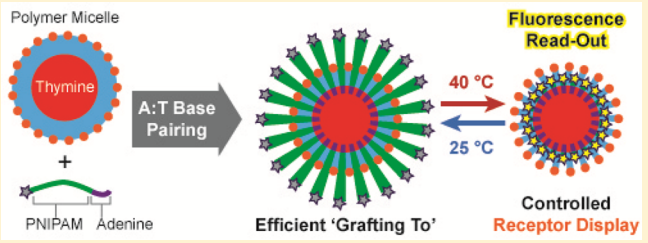

INTRODUCTION

Hydrogen-bonding (H-bonding) mediated assemblies have for many decades been employed as surrogates to mimic the nanostructures formed as a result of nucleobase pairing within RNA and DNA.[1−9] Hydrogen bonds are normally weaker than covalent and ionic bonds, with an energy typically between 5 and 30 kJ mol^{-1}. Importantly, although a single hydrogen bond is weak, controlled display of multiple H-bonding groups can result in strong, specific interactions. Synthetic chemists inspired by Nature have widely utilized complementary H-bonding interactions to achieve templated polymerization,[10−14] mediate polymer tacticity,[15] and tune nanoparticle morphologies.[16−18] Selective recognition of nucleobase functionalities has also provided a new route to modify and functionalize nucleobase- or DNA-containing nanomaterials.[19−23]

Mixed polymer-grafted nanostructures and surfaces, consisting of two distinct polymers in the outer layer, enable various applications such as smart wetting surfaces,[24,25] controllable oil/water separation,[26] and cancer diagnostics.[27] Generally, mixed-corona polymeric nanostructures are made using cooperative self-assembly of two distinct diblock copolymers in a common selective solvent, and then microphase separation can occur due to differences in the properties of the two diblock copolymers.[28,29] Alternatively, two "grafting" strategies can be exploited to attach polymer chains to the surface of a nanostructure: (i) "grafting from" and (ii) "grafting to" approaches.[30] In the "grafting from" approach, polymer chains are formed from initiator-functionalized nanostructures/surfaces, which can produce thick and very dense polymer layers.[31] However, stringent reaction conditions and complicated purification steps often limit potential applications. On the other hand, the relatively simple "grafting to" strategy involves the attachment of prefabricated polymers via either physisorption[32] or covalent bond formation.[30,33−36] Typically, the "grafting to" strategy suffers from several limitations. With increasing polymer molecular weight, the reaction efficiency between the end-group and the reactive group on the surface significantly decreases.[37] Furthermore, steric repulsion between polymer chains is expected to hinder the successful fabrication of novel polymeric materials due to relatively low grafting densities.

The "grafting to" strategy also has some undoubted advantages. Tethered polymers can be thoroughly characterized prior to conjugation, which allows the fabrication of tailor-made

Received: February 8, 2017
Revised: March 22, 2017
Published: April 18, 2017

DOI: 10.1021/acs.macromol.7b00286
Macromolecules 2017, 50, 3662−3670

nanostructures or surfaces.[38,39] Furthermore, the "grafting to" approach is experimentally very straightforward, unlike the "grafting from" approach. Since the development of "click" chemistry in the past decade, a range of modular conjugation strategies have breathed new life into "grafting to" approaches.[40,41] However, the relatively small and mostly buried reactive groups of long polymer chains often result in moderate grafting densities and require high reactant concentrations.[42,43]

Stimuli-responsive polymers represent a growing cadre of materials that support various applications such as responsive coatings and controlled release agents.[44] Many smart polymers have been developed to switch their various functions via external stimuli such as pH, light, temperature, etc.[45−50] Such switching behavior has been utilized to turn off/on activity or interaction of functional groups within the material. For example, switching of a cationic *N*,*N*-dimethyl-2-morpholinone (CD-Ring) film between attacking and defending against bacteria, through a change in solution pH, has been achieved in a controlled manner.[45] Furthermore, light-responsive azobenzene[46] and thermoresponsive PNIPAM[49,50] have been utilized to reversibly conceal and expose ligand for biospecific cell adhesion or targeting.

Recent work in our group has highlighted the effect of complementary multiple H-bonding interactions within the core of self-assembled nanostructures on their self-assembly behavior.[17] Indeed, the utilization of specific complementary A−T interactions within the micelle cores enabled the progressive modulation of nanostructure morphology. At high dilution (0.5 mg mL^{-1}), efficient complementary interactions allowed for control over nanostructure morphology. To expand on the utility and application of these discoveries, we aimed to exploit the complementary interactions within the nanostructure cores to allow for the preparation of responsive mixed-corona micelles. Our previous work employed PNAM as the sole hydrophilic block and thus generated micelles with a homogeneous and non-responsive corona. In contrast, our new system uses both hydrophilic PNAM and PNIPAM in different diblock copolymers, thus forming a mixed corona micelle. Mixed-corona micelles containing both thermoresponsive PNIPAM, which can reversibly manipulate the micelle surface functionality, and a permanently hydrophilic, non-responsive PNAM, which was able to stabilize the nanoparticles above the characteristic cloud point of PNIPAM,[51] were prepared using a "grafting to" approach. This approach allowed facile control of nanostructure size through the introduction of complementary diblock copolymers, poly(*N*-isopropylacrylamide)-*b*-poly(3-(adenine-9-yl)propylacrylamide) (PNIPAM-*b*-PAAm) with different chain lengths, to preformed micelles with thymine-functionalized cores. Interestingly, the thermoresponsive polymeric micelles exhibited behavior consistent with single particle collapse/swelling, and the transition was fully reversible. Introduction of an environmentally sensitive fluorophore at the chain ends of the hydrophilic blocks using a "grafting to" approach allowed the hydrophobicity of the corona domain of the micelles to be probed at different temperatures. Having confirmed the reversible collapse/swelling of the thermoresponsive chains of the corona, it was then demonstrated that it was possible to selectively display or conceal a protein ligand using temperature as a responsive trigger. This work demonstrates that a "grafting to" approach, mediated by complementary nucleobase interactions, allows for the efficient functionalization of polymeric nanostructures/surfaces and represents an efficient route to fabricate tailor-made nanomaterials.

EXPERIMENTAL SECTION

Materials. 2,2′-Azobis(isobutyronitrile) (AIBN) was obtained from Molekula and recrystallized from methanol. 2,2′-Azobis[2-(2-imidazolin-2-yl)propane] dihydrochloride (VA-044, Wako) was used without further purification. Concanavalin A (Con A) was used as purchased from Sigma-Aldrich. 4-Acryloylmorpholine (NAM) was bought from Sigma-Aldrich and was purified by vacuum distillation. *N*-Isopropylacrylamide (NIPAM) was purchased from Sigma-Aldrich and recrystallized from a toluene−hexane mixture prior to use. 3-(Adenine-9-yl)propylacrylamide (AAm), 3-(thymin-1-yl)propylacrylamide (TAm), 2-(((butylthio)carbonothiolyl)thio)propanoic acid, and micelle **M1** were synthesized as described previously[17] and stored at 4 °C. DMF, DMSO, and other chemicals were obtained from Fisher Chemicals and used without further purification. Dry solvents were obtained by passing over a column of activated alumina using an Innovative Technologies solvent purification system. Dialysis membranes (MWCO = 3.5 kDa) were purchased from Spectra/Por.

Instrumentation. ^{1}H NMR and ^{13}C NMR spectra were recorded on a Bruker DPX-300, DPX-400, or HD500 spectrometer with DMSO-d_6 or $CDCl_3$ as the solvent. The chemical shifts of protons were relative to tetramethylsilane (TMS) at δ = 0 ppm when using $CDCl_3$ or solvent residues (DMSO 2.50 ppm). UV−vis spectra were recorded on a PerkinElmer Lambda 35 UV−vis instrument. Turbidimetry assays were performed as described in a previous publication.[52] Fluorescence spectra were recorded using an Agilent Cary Eclipse fluorescence spectrophotometer. The samples were incubated at the relevant temperatures for at least 2 min and then measured immediately. High-resolution mass spectrometry (HR-MS) was conducted on a Bruker UHR-Q-TOF MaXis with electrospray ionization (ESI). Size exclusion chromatography (SEC) data were obtained in HPLC grade DMF containing 5 mM NH_4BF_4 at 50 °C, with a flow rate of 1.0 mL min^{-1}, on a set of two PLgel 5 μm Mixed-D columns and a guard column. SEC data were analyzed with Cirrus SEC software calibrated using poly(methyl methacrylate) (PMMA) standards.

Hydrodynamic diameters (D_h) and size distributions of the self-assemblies were determined by dynamic light scattering (DLS). The DLS instrumentation consisted of a Malvern Zetasizer NanoS instrument with a 4 mW He−Ne 633 nm laser module. Measurements were made at a detection angle of 173°, and Malvern DTS 7.03 software was used to analyze the data. D_h was calculated by fitting the apparent diffusion coefficient in the Stokes−Einstein equation $D_h = kT/(3\pi\eta D_{app})$, where k, T, and η are the Boltzmann constant, the temperature, and the viscosity of the solvent, respectively. As the measured sample is a solution of monodispersed spherical micelles, D_h coincides to the real hydrodynamic diameter as D_{app} is equal to the translational diffusion coefficient (D_t). For thermoresponsive size change, all measurements were run at least three times with a minimum of 10 runs per measurement for every temperature point. For reversible size change, the samples were incubated at the relevant temperature for 2 min before measurement. Static light scattering (SLS) measurements were conducted with an ALV CGS3 (λ = 632 nm) at different temperatures. The data were collected from 50° to 150° with an interval of 10° against a toluene standard. The self-assembled solutions were filtered through 0.45 μm nylon filters prior to analysis.

TEM observations were performed on a JEOL 2000FX electron microscope at an acceleration voltage of 200 kV. TEM samples were prepared by drop deposition of an aqueous solution onto a copper grid coated with Formvar. Generally, a drop of sample (10 μL) was pipetted on a grid, left for several minutes, and then blotted away. Uranyl acetate (UA, 1%) was used for the staining of TEM samples. TEM images were analyzed using the ImageJ software package, and over 100 particles were counted for each sample to obtain number-average diameter D_n (for spherical micelles).

DOI: 10.1021/acs.macromol.7b00286
Macromolecules 2017, 50, 3662−3670

Synthesis of Poly(*N*-isopropylacrylamide) (PNIPAM) Macro-CTA via RAFT Polymerization. The typical procedure was as follows: a 10 mL ampule was charged with NIPAM (339.5 mg, 3.0 mmol), 2-(((butylthio)carbonothiolyl)thio)propanoic acid (2.4 mg, 0.01 mmol), AIBN (0.16 mg, 0.001 mmol), and 1,4-dioxane (0.68 mL). The mixture was thoroughly degassed via four freeze–pump–thaw cycles, filled with nitrogen, and then immersed in an oil bath at 70 °C for 2 h. The conversion was determined by ^{1}H NMR spectroscopy. The polymerization solution was then precipitated three times from cold diethyl ether. The light yellow polymer was dried in a vacuum oven overnight at room temperature and analyzed by ^{1}H NMR spectroscopy and DMF SEC.

Synthesis of PNIPAM$_x$-*b*-PAAm$_y$ Diblock Copolymers. The typical procedure was as follows. For PNIPAM$_{262}$-*b*-PAAm$_{20}$: PNIPAM$_{262}$ (75 mg, 0.0025 mmol), AAm (15.4 mg, 0.0625 mmol), and AIBN (0.04 mg, 0.00025 mmol) were dissolved in DMSO (0.3 mL). The mixture was thoroughly degassed via four freeze–pump–thaw cycles, filled with nitrogen, and then immersed in an oil bath at 70 °C overnight. An aliquot of the crude product was taken and analyzed by ^{1}H NMR spectroscopy to calculate the conversion. The residual solution was precipitated three times from cold CH_3OH. The light yellow polymer was dried in a vacuum oven overnight at room temperature and analyzed by ^{1}H NMR spectroscopy and DMF SEC. The synthetic details and characterization of the fluorescent ABM and D-mannose containing CTAs can be found in the Supporting Information (Figures S1–S4, Schemes S1 and S2).

Self-Assembly of PNAM$_{98}$-*b*-PTAm$_{302}$ P10 Diblock Copolymer in Water. The diblock PNAM$_{98}$-*b*-PTAm$_{302}$ **P10** was synthesized using a D-mannose containing CTA (Figure S4). For the self-assembly of **P10**, a solvent switch method was used. Specifically, the diblock copolymer was dissolved in DMF (at 8 mg mL^{-1}) and stirred for 2 h. Then an excess of 18.2 MΩ·cm water was added via a syringe pump at a rate of 1 mL h^{-1}. The final volume ratio between water and organic solvent was 8:1. The solution was then dialyzed against 18.2 MΩ·cm water (MWCO = 3.5 kDa), incorporating at least six water changes, to afford self-assemblies (**M10**) at a concentration of ca. 1 mg mL^{-1}.

Preparation of Mixed-Corona Micelles Containing PNIPAM-*b*-PAAm and PNAM-*b*-PTAm. Diblock copolymers PNIPAM$_x$-*b*-PAAm$_y$ **P2–P9** were dissolved in H_2O at 10 mg mL^{-1}. This was then added to the micellar solution of **M1** or **M10** (0.5 mg mL^{-1}) dropwise with stirring. The molar ratios were calculated according to the M_n determined from ^{1}H NMR spectroscopic analyses and the polymer mass concentration. The mixture was then sealed and allowed to stir at room temperature for at least 2 h. The solutions were then analyzed by DLS, TEM, and SLS.

RESULTS AND DISCUSSION

Synthesis of Mixed-Corona Micelles through a Supramolecular "Grafting To" Approach. A diblock copolymer, **P1**, with a permanently hydrophilic domain and a thymine functional hydrophobic block was prepared by RAFT polymerization. The self-assembly of this diblock copolymer was achieved via a solvent switch method as reported previously to afford micelle **M1** (D_h = 69 nm, PD = 0.058) at ca. 1 mg mL^{-1}. In order to fabricate mixed-corona micelles using a "grafting to" approach a series of PNIPAM-*b*-PAAm diblock copolymers with various hydrophilic block lengths were also prepared via RAFT polymerization (Table 1, **P2–P5**, Figures S5 and S6). Subsequently, 1 mol equiv. of complementary diblock copolymers **P2–P5** in water was added to the solution of micelle **M1** with stirring at room temperature and left for at least 2 h. In agreement with our previous work, no morphology transition or disassembly occurred when only 1 mol equiv. of complementary diblock copolymers was added to the preformed micelles.[17] Using this approach, well-defined mixed-corona micelles **M2–M5** were formed through multiple H-bonding interactions between the thymine-containing micelle core of **M1** and complementary adenine-containing diblock copolymers **P2–P5** (Scheme 1 and Figures S7a–S10a).

Table 1. Characterization Data of Polymers P1–P10

Polymer	Structure	$M_{n,NMR}$ [a] (kDa)	$M_{n,SEC}$ [b] (kDa)	$Đ_M$ [b]
P1	PNAM$_{96}$-*b*-PTAm$_{301}$	85.1	68.4	1.29
P2	PNIPAM$_{96}$-*b*-PAAm$_{20}$	15.5	17.8	1.05
P3	PNIPAM$_{176}$-*b*-PAAm$_{20}$	25.3	23.9	1.10
P4	PNIPAM$_{262}$-*b*-PAAm$_{20}$	35.3	34.1	1.13
P5	PNIPAM$_{438}$-*b*-PAAm$_{20}$	56.7	52.9	1.18
P6	PNIPAM$_{262}$	29.9	31.6	1.09
P7	PNAM$_{295}$-*b*-PAAm$_{20}$	47.0	36.8	1.17
P8	PNIPAM$_{237}$-*b*-PAAm$_{20}$ [c]	33.0	32.8	1.17
P9	PNAM$_{244}$-*b*-PAAm$_{20}$ [c]	40.5	33.0	1.25
P10	PNAM$_{98}$-*b*-PTAm$_{302}$ [d]	85.8	64.2	1.32

[a]Determined by ^{1}H NMR spectroscopy (400 MHz) in deuterated DMSO. [b]Determined by DMF SEC, with poly(methyl methacrylate) (PMMA) standards. [c]Aminobromomaleimide-containing chain transfer agent (CTA) was used. [d]D-mannose containing CTA was used.

Mixed-corona micelles generally inherit the solution properties of both corona-forming blocks. Indeed, dynamic light scattering (DLS) analysis indicated that the PNIPAM chains in the mixed-corona micelles collapsed, and no aggregation between self-assembled nanostructures was observed at 60 °C (see Figures S7b–S10b). For example, Figure 1a shows the heating process for **M4** and the resulting hydrodynamic diameter of the mixed-corona micelles, which decreased from ca. 89 to ca. 70 nm upon heating from 15 to 60 °C. Meanwhile, the polydispersity values of the mixed-corona micelles were determined to lie in a range of 0.02–0.08 during this heating process. Micelle **M4** solution was dried and stained with uranyl acetate at 20 and 60 °C for TEM imaging (Figures 1b and 1c, respectively). TEM images further suggested that no aggregation was observed at 60 °C. Meanwhile, smaller spherical nanoparticles with diameter ca. 61 nm were observed at 60 °C compared with spherical nanoparticles with diameter ca. 70 nm at 20 °C. This further suggested that these "grafting to" mixed-corona micelles underwent intraparticle chain collapse without interparticle aggregation. In stark contrast, upon addition of 1 mol equiv. of PNIPAM **P6** without a complementary nucleobase block to preformed micelle **M1**, large aggregates and much higher dispersity values were observed by DLS for the resultant micelle, **M6**, above the cloud point of the PNIPAM block (Scheme 1 and Figure S11a). Notably, complementary diblock copolymers **P2–P5** with small anchoring groups avoided the formation of frozen aggregates and facilitated efficient incorporation of the complementary diblock copolymers. Static light scattering (SLS) analyses of micelle **M4** also indicated no appreciable change in the apparent molecular weight by light scattering (M_w) and aggregation number (N_{agg}) of the respective micelles at 15, 35, and 50 °C (Figure S12).[55] On the basis of these initial results, we proposed that the size change of the mixed-corona micelle upon heating was a result of PNIPAM collapse with retention of the micellar structure rather than disassembly and re-formation of the micellar aggregates (Scheme 1). As expected, the hydrophilic PNAM chains were still capable of stabilizing mixed-corona micelles even when the PNIPAM chains were fully collapsed at elevated temperatures.

Given that H-bonding interactions are known to be disrupted at elevated temperatures, we next investigated the effect of

DOI: 10.1021/acs.macromol.7b00286
Macromolecules 2017, 50, 3662–3670

Scheme 1. Syntheses of Mixed-Corona Polymeric Nanostructures M2−M7 through a Supramolecular "Grafting To" Approach Mediated by Complementary Nucleobase Interactions

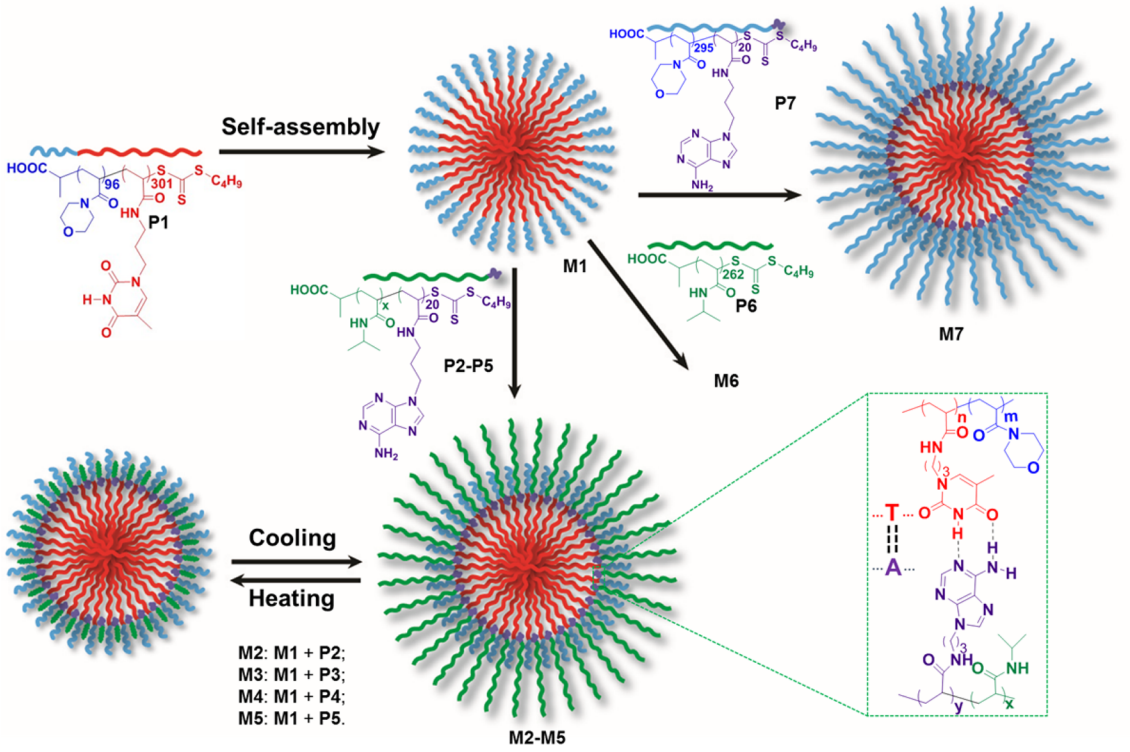

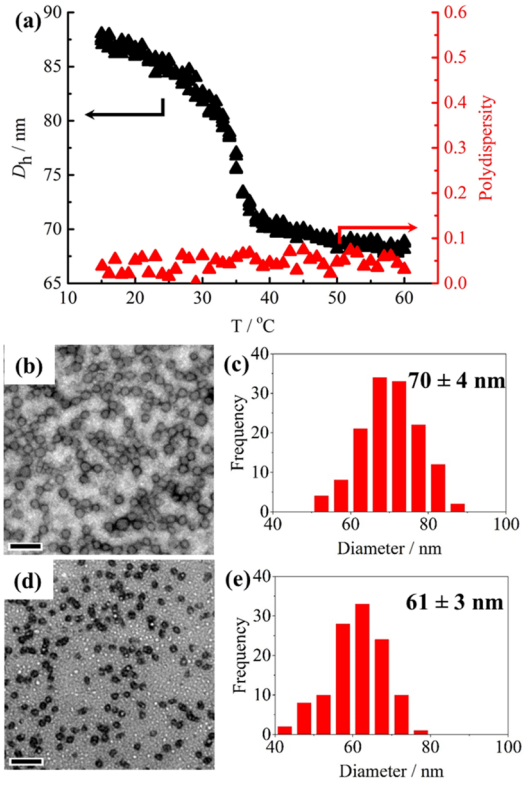

Figure 1. (a) Variation of the hydrodynamic diameter (D_h) of the mixed-corona micelles **M4** with temperature as determined by DLS; TEM images (stained with uranyl acetate) and histograms of number-average diameter distribution of **M4** at (b, c) 20 °C and (d, e) 60 °C. Scale bar: 200 nm.

temperature on PNAM corona micelles prepared by a "grafting to" approach through the addition of a non-responsive diblock copolymer, **P7** ($PNAM_{295}$-*b*-$PAAm_{20}$), to the preformed micelle **M1** (Scheme 1). The resultant micelle **M7** was investigated by temperature-dependent DLS, and no appreciable size change was observed at elevated temperatures, which demonstrated the stability of the H-bonding interactions in the micellar core up to 60 °C (Figure S11b). This result also suggested that the size decrease observed in the mixed-corona micelles **M2−M5** were solely caused by the intraparticle PNIPAM chain collapsing rather than the separation of complementary polymer chains at elevated temperatures.

Reversible Alteration of the Sizes of Mixed-Corona Nanoparticles. The size of a nanoparticle is an important parameter that affects the majority of applications but perhaps most notably their application in nanomedicine. In biomedical delivery applications, nanoparticle sizes greatly influence their circulation time, rate of clearance, selective tissue distribution, and intracellular fate.[54] To circumvent the need for laborious syntheses to access nanoparticles of a particular size, the "grafting to" strategy described here provides a facile method to prepare nanoparticles of controlled sizes. Indeed, we have demonstrated that a series of nanoparticles with different sizes (75−110 nm) could be easily produced by adding complementary diblock copolymers with different chain lengths to a single preformed micelle (**M1** of a small size 69 nm). Moreover, the composition and properties of the newly formed nanoparticles could be adjusted by changing the chemistry of the added complementary block copolymers.

To demonstrate this approach, 1 mol equiv. of complementary diblock copolymers **P2−P5** was added to separate solutions of preformed micelle **M1**. Hydrodynamic diameters of the resultant nanoparticles were observed to increase stepwise from ca. 69 nm for **M1** to ca. 75 nm for **M2** and then to ca. 110

DOI: 10.1021/acs.macromol.7b00286
Macromolecules 2017, 50, 3662−3670

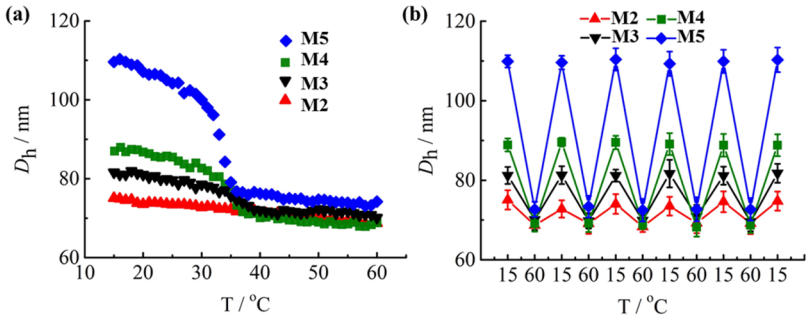

Figure 2. (a) DLS analyses of the mixed-corona micelles **M2**−**M5** with different PNIPAM chain lengths heated from 15 to 60 °C. (b) Reversible size change (D_h) of mixed-corona micelles **M2**−**M5** at both 15 and 60 °C. Error bars show size dispersity (PD).

Scheme 2. Syntheses of ABM-Functionalized PNIPAM$_{237}$-*b*-PAAm$_{20}$ [P8] and Subsequent Addition to M1 To Afford Mixed Micelles M8, and D-Mannose-Functionalized PNAM$_{98}$-*b*-PTAm$_{302}$ [P10] and Subsequent Assembly To Afford Micelles M10 and Mixed Micelles, M11

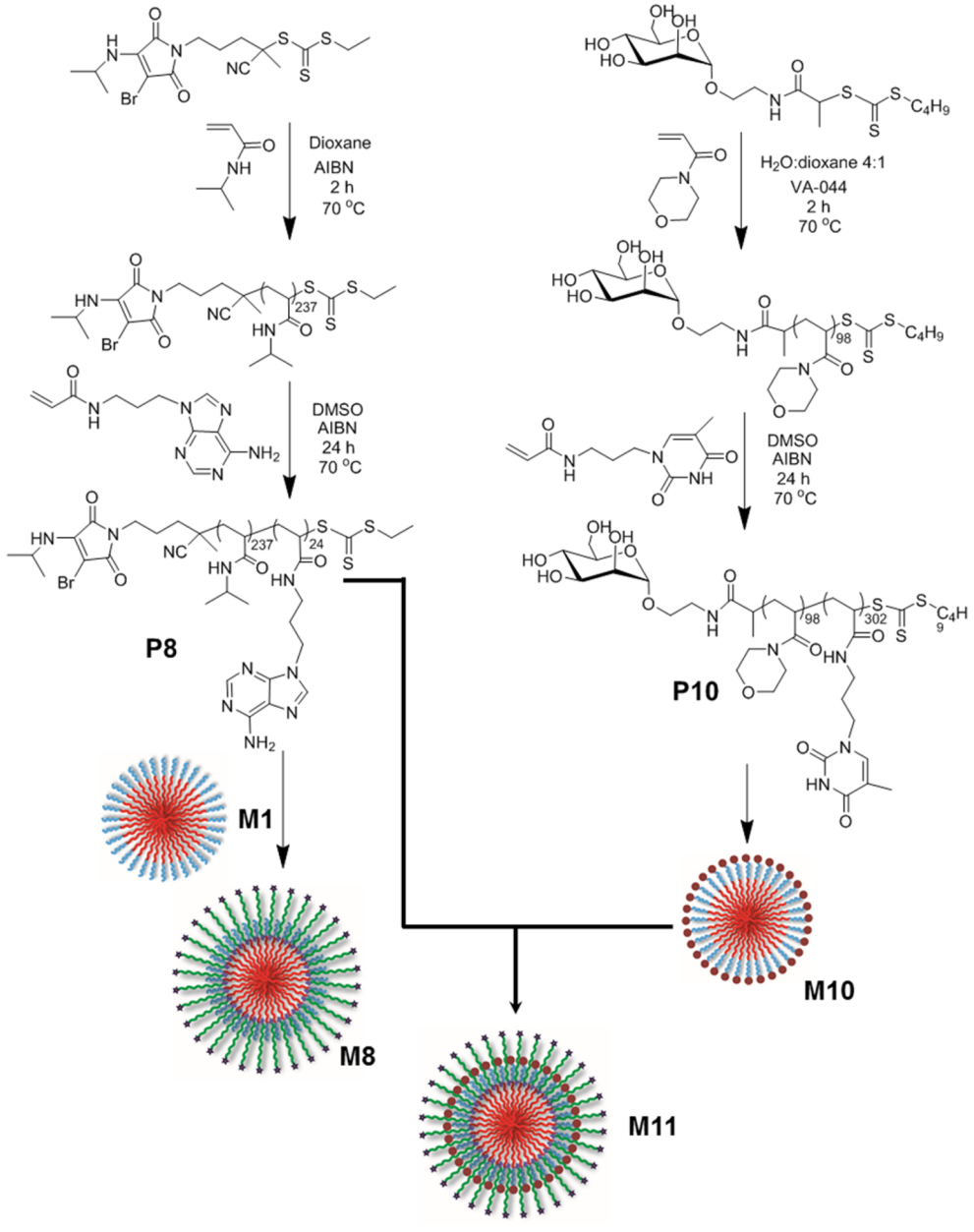

DOI: 10.1021/acs.macromol.7b00286
Macromolecules 2017, 50, 3662−3670

nm for **M5**. We propose that this increase was due to the increase in PNIPAM chain lengths in the added complementary diblock copolymers. Upon heating of the mixed-corona micelle solutions, the PNIPAM chains appeared to gradually collapse up to their cloud point at 32 °C (Figure 2a). Above 40 °C, there was no further size alteration observed by DLS analysis. It is notable that mixed-corona micelles **M2**−**M5** all collapsed to micelles of similar sizes (70−74 nm in hydrodynamic diameter) at 60 °C. We presumed that this was because the collapsed PNIPAM chains at elevated temperatures resided at the core−corona interface and therefore played a negligible role in determining the mixed-corona micelles' hydrodynamic diameters.

For thermoresponsive nanoparticles, fast and fully reversible switching behavior is of great importance.[55−57] As shown in Figure 2b, size switching of the mixed-corona micelles could be performed for at least five heating and cooling cycles, highlighting that this transition was fully reversible. More importantly, the transition could be achieved in just 2 min as determined by DLS analysis. We propose that the distribution of both thermoresponsive PNIPAM chains and non-responsive PNAM chains in the mixed micelle corona led to less chain entanglement and as a result a faster transition compared with micelles which have only a PNIPAM corona domain.[55,56] Therefore, the "grafting to" mixed nature of the micelle coronas resulted in cooperative effects—nanoparticles were stabilized and the speed of the coronal collapse increased. The dispersity of the nanoparticles at both high and low temperatures remained below 0.1 throughout the five cycles. Hence, we propose that at low temperatures the elongated PNIPAM chains served as the outer corona and stabilized the large mixed micelles. Then at high temperatures, the smaller mixed micelles remained stabilized by the hydrophilic PNAM chains, which were revealed as a result of the collapse of PNIPAM chains to the core−corona interface.

Altering the Coronas and Surfaces of Mixed-Corona Nanoparticles. Changes in the surface chemistry of nanostructures can be used to modulate hydrophilicity, cellular uptake, and endocytosis.[49] However, it is difficult to probe a nanoparticle surface's chemistry and local environment. Recent work in our group has reported the development of aminobromomaleimide (ABM) and dithiolmalemide (DTM) fluorophores.[58,59] These are a new class of highly emissive compounds which can be readily incorporated into micellar constructs without noticeable effects on the particle size or dynamics.[60,61] Interestingly, these fluorophores show much lower emission in water compared with more hydrophobic environments and a concentration independent emission maximum.[62] We therefore proposed that ABMs could be used as a probe to provide a fluorescence read-out of the hydrophobicity of the fluorophore's local environment.[63] In the present case, it was envisaged that ABMs could be used to reveal the hydration state of the coronal domain of the mixed-corona micelles.

Fluorescent diblock copolymer PNIPAM$_{237}$-*b*-PAAm$_{20}$ **P8** was synthesized (as described for **P2**−**P5**) and added to preformed micelle **M1** to yield the mixed-corona micelle **M8** (Scheme 2 and Table 1). A clear fluorescence emission peak at 488 nm (λ_{ex} = 350 nm) was observed at 40 °C (when the PNIPAM coronal chain was collapsed and hydrophobic in nature), which was attributed to the fluorescence emission of the ABM fluorophore in a hydrophobic environment (Figure 3a). This fluorescence emission peak was no longer present at

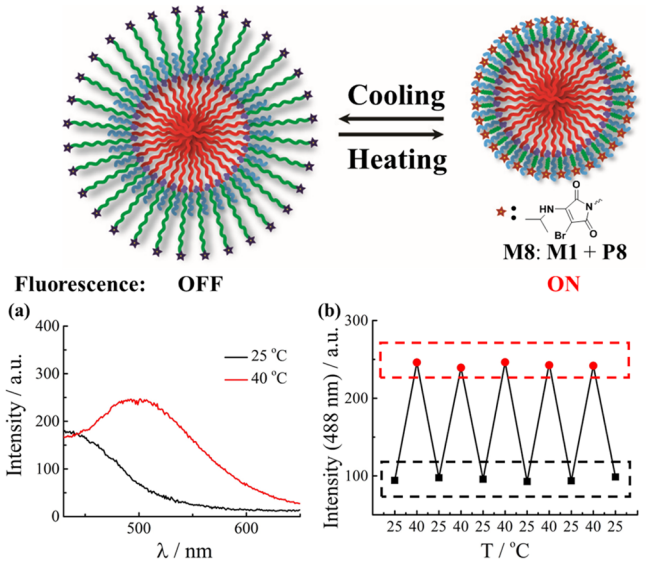

Figure 3. Demonstration of a reversible fluorescence ON/OFF switch using ABM-tagged mixed-corona nanoparticles. (a) Fluorescence spectra (λ_{ex} = 350 nm) of mixed-corona micelle **M8** at 25 (black) and 40 °C (red). (b) Fluorescence emission intensity of **M8** at 488 nm at 25 and 40 °C for five consecutive heating and cooling cycles (λ_{ex} = 350 nm).

25 °C as the elongated PNIPAM resulted in ABM being brought into a more hydrophilic environment, which led to fluorescence quenching. Note that the shoulder peak at 430 nm (in Figure 3a) appeared as a result of scattering of the micelle solution. A control experiment using micelle **M4** (which did not contain the ABM functionality) displayed a slight decrease in the shoulder peak at 40 °C (Figure S13a), which can be rationalized by assuming that the collapsing nanostructures at 40 °C contributed to less scattering due to their smaller size. Moreover, the non-responsive corona micelle **M9** consisting of preformed micelle **M1** and ABM-functionalized PNAM$_{244}$-*b*-PAAm$_{20}$ **P9** exhibited no appreciable fluorescence change at 25 and 40 °C, as the fluorophore did not undergo any significant microenvironment change as the hydrophobicity of the coronal block did not change at elevated temperature (Figure S13b). A similar fluorescence read-out response was observed for the mixed micelle consisting of micelle **M1** and ABM-attached PNIPAM$_{40}$-*b*-PAAm$_{20}$ (see Figure S13c). Hence, the fluorescence read-out of the ABM mixed micelles was proposed to be determined by the hydrophobic microenvironment where the dye lies and hence is independent of PNIPAM corona block length. We concluded that the fluorescence ON/OFF switch was triggered by changes in the microenvironment surrounding the ABM fluorophore upon collapse of the responsive block—this enabled a read-out of the surface state of the mixed corona micelles. Again, as suggested by DLS analysis and as shown in Figure 3b, the temperature-dependent fluorescence switch was fully reversible. The intensity of the fluorescence emission peak at 488 nm at 40 °C did not decrease, even after five cycles of heating and cooling, which indicated that collapse and expansion of the PNIPAM did not lead to any loss of micelle structure and confirmed the integrity of the nucleobase interactions within the core domain during these heat−cool cycles.

We next explored the utility of this "grafted to" system in controlling protein ligand display on the mixed micelle surface using changes in temperature. To achieve this, we utilized

DOI: 10.1021/acs.macromol.7b00286
Macromolecules 2017, 50, 3662−3670

Concanavalin A (Con A), a tetrameric mannose-binding plant lectin, which can effectively bind to the ligand D-mannose with moderate binding constants.[64] This type of specific recognition between carbohydrates and proteins is involved in many complex cellular events, including cell adhesion, pathogen invasion, and cancer metastasis, to name but a few.[65] D-Mannose-functionalized $PNAM_{98}$-*b*-$PTAm_{302}$ **P10** was synthesized and self-assembled to form non-responsive micelle **M10** as an experimental control (Scheme 2 and Figure S14a). In addition, D-mannose containing mixed-corona micelles **M11** were prepared by adding diblock copolymer **P8** to preformed micelle **M10** (Scheme 2 and Figure S14b) as described for the previous mixed micellar systems. This afforded a micelle **M11** with a mixed-corona domain, which consisted of a responsive PNIPAM block bearing the ABM probe and a non-responsive PNAM block bearing the ligand, which we proposed could be selectively revealed and buried depending on the state of the responsive block (i.e. the temperature of the system). To explore this, a Con A agglutination assay was used to measure the extent of binding between Con A and **M11**.[52] At 25 °C, the D-mannose ligands were expected to be fully concealed by the extended PNIPAM chains, and indeed no agglutination was observed at this temperature (Figure 4a). In contrast, at 40 °C

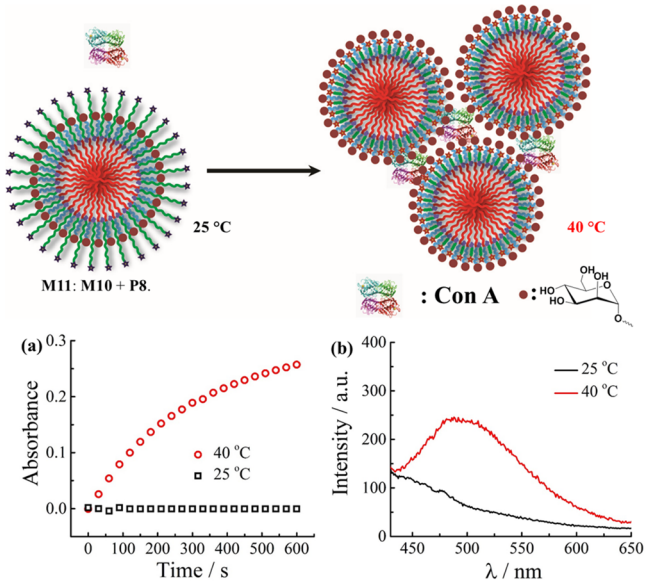

Figure 4. Controlled ligand display on the mixed-corona micelle surface. (a) Agglutination assay of mixed-corona micelle **M11** with Con A at 25 and 40 °C. (b) Fluorescence spectra of **M11** at 25 and 40 °C (λ_{ex} = 350 nm).

significant agglutination was observed—at this temperature the PNIPAM chains were expected to collapse, revealing the ligands for binding with the Con A receptors. Notably, the binding between the receptor D-mannose and Con A is not reversible, and the formed aggregates precipitated out after longer time periods. Further analysis of the ABM-tagged mixed-corona micelle **M11** using fluorescence spectroscopy confirmed the collapse of the PNIPAM above 40 °C, with the characteristic change in the emission spectrum of ABM again observed (Figure 4b).

CONCLUSIONS

In summary, a novel supramolecular "grafting to" strategy for the formation of well-defined mixed-corona micelles has been demonstrated. This strategy involved the exploitation of multiple complementary H-bonding interactions between thymine-containing cores of preformed micelles and added adenine-containing diblock copolymers. Polymeric micelles with different sizes were easily prepared by changing the chain lengths of the added complementary diblock copolymers. Intraparticle chain collapse allowed micelle size and coronal state to be reversibly altered in response to an external stimulus—in this case temperature—and this could be coupled to the reversible display/concealment of protein ligands at the nanoparticle surface. While in this work a temperature responsive block was utilized to showcase the viability of this approach for achieving the reversible presentation of functionality at the surface of a nanoparticle, other stimuli responses could be easily utilized such as pH, light, etc. Indeed, through the synthesis of the appropriate complementary diblock copolymers, the incorporation of a diverse range of functionalities at the nanoparticle surface can be envisaged using this supramolecular "grafting to" approach. This work provides a new route and platform to fabricate mixed polymer-grafted nanostructures and surfaces, which may find potential applications as smart materials for utilization in a range of areas such as nanomedicine.

ASSOCIATED CONTENT

Supporting Information

The Supporting Information is available free of charge on the ACS Publications website at DOI: 10.1021/acs.macromol.7b00286.

Synthetic details of ABM-containing and D-mannose-containing CTA, ^{1}H NMR spectra, SEC traces of nucleobase-containing diblock copolymers, and DLS, SLS, and fluorescence characterization of mixed-corona micelles (PDF)

AUTHOR INFORMATION

Corresponding Author

*E-mail r.k.o-reilly@warwick.ac.uk; Fax +44 024 7652 4112; Tel +44 024 7652 3236 (R.K.O.).

ORCID

Guosong Chen: 0000-0001-7089-911X

Rachel K. O'Reilly: 0000-0002-1043-7172

Notes

The authors declare no competing financial interest.

ACKNOWLEDGMENTS

The authors thank the University of Warwick, China Scholarship Council (Z.H.), NSFC (nos. 21474020 and 91527305), EPSRC, and the ERC (grant 615142) for research funding.

REFERENCES

(1) Peters, G. M.; Davis, J. T. Supramolecular Gels Made from Nucleobase, Nucleoside and Nucleotide Analogs. *Chem. Soc. Rev.* **2016**, *45*, 3188–3206.

(2) Krieg, E.; Bastings, M. M.; Besenius, P.; Rybtchinski, B. Supramolecular Polymers in Aqueous Media. *Chem. Rev.* **2016**, *116*, 2414–2477.

DOI: 10.1021/acs.macromol.7b00286
Macromolecules 2017, 50, 3662–3670

(3) McHale, R.; O'Reilly, R. K. Nucleobase Containing Synthetic Polymers: Advancing Biomimicry via Controlled Synthesis and Self-Assembly. *Macromolecules* **2012**, *45*, 7665−7675.
(4) Mather, B. D.; Baker, M. B.; Beyer, F. L.; Green, M. D.; Berg, M. A. G.; Long, T. E. Multiple Hydrogen Bonding for the Noncovalent Attachment of Ionic Functionality in Triblock Copolymers. *Macromolecules* **2007**, *40*, 4396−4398.
(5) Zhang, K.; Talley, S. J.; Yu, Y. P.; Moore, R. B.; Murayama, M.; Long, T. E. Influence of Nucleobase Stoichiometry on the Self-Assembly of ABC Triblock Copolymers. *Chem. Commun.* **2016**, *52*, 7564−7567.
(6) Lutz, J.-F.; Thunemann, A. F.; Rurack, K. DNA-Like Melting of Adenine- and Thymine-Functionalized Synthetic Copolymers. *Macromolecules* **2005**, *38*, 8124−8126.
(7) Spijker, H. J.; van Delft, F. L.; van Hest, J. C. M. Atom Transfer Radical Polymerization of Adenine, Thymine, Cytosine, and Guanine Nucleobase Monomers. *Macromolecules* **2007**, *40*, 12−18.
(8) Zhang, K.; Aiba, M.; Fahs, G. B.; Hudson, A. G.; Chiang, W. D.; Moore, R. B.; Ueda, M.; Long, T. E. Nucleobase-Functionalized Acrylic ABA Triblock Copolymers and Supramolecular Blends. *Polym. Chem.* **2015**, *6*, 2434−2444.
(9) Romulus, J.; Weck, M. Single-Chain Polymer Self-Assembly Using Complementary Hydrogen Bonding Units. *Macromol. Rapid Commun.* **2013**, *34*, 1518−1523.
(10) Khan, A.; Haddleton, D. M.; Hannon, M. J.; Kukulj, D.; Marsh, A. Hydrogen Bond Template-Directed Polymerization of Protected 5′-Acryloylnucleosides. *Macromolecules* **1999**, *32*, 6560−6564.
(11) South, C. R.; Weck, M. Template-Enhanced Ring-Opening Metathesis Polymerization. *Macromolecules* **2007**, *40*, 1386−1394.
(12) Lo, P. K.; Sleiman, H. F. Nucleobase-Templated Polymerization: Copying the Chain Length and Polydispersity of Living Polymers into Conjugated Polymers. *J. Am. Chem. Soc.* **2009**, *131*, 4182−4183.
(13) McHale, R.; Patterson, J. P.; Zetterlund, P. B.; O'Reilly, R. K. Biomimetic Radical Polymerization via Cooperative Assembly of Segregating Templates. *Nat. Chem.* **2012**, *4*, 491−497.
(14) Milnes, P. J.; McKee, M. L.; Bath, J.; Song, L.; Stulz, E.; Turberfield, A. J.; O'Reilly, R. K. Sequence-Specific Synthesis of Macromolecules Using DNA-Templated Chemistry. *Chem. Commun.* **2012**, *48*, 5614−5616.
(15) Tao, Y.; Satoh, K.; Kamigaito, M. Nucleobase-Mediated Stereospecific Radical Polymerization and Combination with RAFT Polymerization for Simultaneous Control of Molecular Weight and Tacticity. *Macromol. Rapid Commun.* **2011**, *32*, 226−232.
(16) Kang, Y.; Pitto-Barry, A.; Rolph, M. S.; Hua, Z.; Hands-Portman, I.; Kirby, N.; O'Reilly, R. K. Use of Complementary Nucleobase-Containing Synthetic Polymers to Prepare Complex Self-Assembled Morphologies in Water. *Polym. Chem.* **2016**, *7*, 2836−2846.
(17) Hua, Z.; Pitto-Barry, A.; Kang, Y.; Kirby, N.; Wilks, T. R.; O'Reilly, R. K. Micellar Nanoparticles with Tuneable Morphologies through Interactions between Nucleobase-Containing Synthetic Polymers in Aqueous Solution. *Polym. Chem.* **2016**, *7*, 4254−4262.
(18) Ilhan, F.; Galow, T. H.; Gray, M.; Clavier, G.; Rotello, V. M. Giant Vesicle Formation through Self-Assembly of Complementary Random Copolymers. *J. Am. Chem. Soc.* **2000**, *122*, 5895−5896.
(19) Li, Z.; Zhang, Y.; Fullhart, P.; Mirkin, C. A. Reversible and Chemically Programmable Micelle Assembly with DNA Block-Copolymer Amphiphiles. *Nano Lett.* **2004**, *4*, 1055−1058.
(20) Rothemund, P. W. K. Folding DNA to Create Nanoscale Shapes and Patterns. *Nature* **2006**, *440*, 297−302.
(21) Stahl, E.; Martin, T. G.; Praetorius, F.; Dietz, H. Facile and Scalable Preparation of Pure and Dense DNA Origami Solutions. *Angew. Chem., Int. Ed.* **2014**, *53*, 12735−12740.
(22) Thibault, R. J.; Hotchkiss, P. J.; Gray, M.; Rotello, V. M. Thermally Reversible Formation of Microspheres through Non-Covalent Polymer Cross-Linking. *J. Am. Chem. Soc.* **2003**, *125*, 11249−11252.
(23) Wilks, T. R.; Bath, J.; de Vries, J. W.; Raymond, J. E.; Herrmann, A.; Turberfield, A. J.; O'Reilly, R. K. "Giant Surfactants" Created by the Fast and Efficient Functionalization of a DNA Tetrahedron with a Temperature-Responsive Polymer. *ACS Nano* **2013**, *7*, 8561−8572.
(24) Ionov, L.; Minko, S. Mixed Polymer Brushes with Locking Switching. *ACS Appl. Mater. Interfaces* **2012**, *4*, 483−489.
(25) Minko, S.; Muller, M.; Usov, D.; Scholl, A.; Froeck, C.; Stamm, M. Lateral versus Perpendicular Segregation in Mixed Polymer Brushes. *Phys. Rev. Lett.* **2002**, *88*, 035502.
(26) Zhang, L.; Zhang, Z.; Wang, P. Smart Surfaces with Switchable Superoleophilicity and Superoleophobicity in Aqueous Media: Toward Controllable Oil/Water Separation. *NPG Asia Mater.* **2012**, *4*, e8.
(27) Song, J.; Zhou, J.; Duan, H. Self-Assembled Plasmonic Vesicles of SERS-Encoded Amphiphilic Gold Nanoparticles for Cancer Cell Targeting and Traceable Intracellular Drug Delivery. *J. Am. Chem. Soc.* **2012**, *134*, 13458−13469.
(28) Zhang, Z.; Zhou, C.; Dong, H.; Chen, D. Solution-Based Fabrication of Narrow-Disperse ABC Three-Segment and Theta-Shaped Nanoparticles. *Angew. Chem., Int. Ed.* **2016**, *55*, 6182−6186.
(29) Zhao, B.; Zhu, L. Mixed Polymer Brush-Grafted Particles: A New Class of Environmentally Responsive Nanostructured Materials. *Macromolecules* **2009**, *42*, 9369−9383.
(30) Barbey, R.; Lavanant, L.; Paripovic, D.; Schuwer, N.; Sugnaux, C.; Tugulu, S.; Klok, H.-A. Polymer Brushes via Surface-Initiated Controlled Radical Polymerization: Synthesis, Characterization, Properties, and Applications. *Chem. Rev.* **2009**, *109*, 5437−5527.
(31) Patil, R. R.; Turgman-Cohen, S.; Šrogl, J.; Kiserow, D.; Genzer, J. Direct Measurement of Molecular Weight and Grafting Density by Controlled and Quantitative Degrafting of Surface-Anchored Poly(methyl methacrylate). *ACS Macro Lett.* **2015**, *4*, 251−254.
(32) Brandani, P.; Stroeve, P. Adsorption and Desorption of PEO-PPO-PEO Triblock Copolymers on a Self-Assembled Hydrophobic Surface. *Macromolecules* **2003**, *36*, 9492−9501.
(33) Goldmann, A. S.; Barner, L.; Kaupp, M.; Vogt, A. P.; Barner-Kowollik, C. Orthogonal Ligation to Spherical Polymeric Microparticles: Modular Approaches for Surface Tailoring. *Prog. Polym. Sci.* **2012**, *37*, 975−984.
(34) Ohno, K.; Ma, Y.; Huang, Y.; Mori, C.; Yahata, Y.; Tsujii, Y.; Maschmeyer, T.; Moraes, J.; Perrier, S. Surface-Initiated Reversible Addition−Fragmentation Chain Transfer (RAFT) Polymerization from Fine Particles Functionalized with Trithiocarbonates. *Macromolecules* **2011**, *44*, 8944−8953.
(35) Olivier, A.; Meyer, F.; Raquez, J.-M.; Damman, P.; Dubois, P. Surface-Initiated Controlled Polymerization as a Convenient Method for Designing Functional Polymer Brushes: From Self-Assembled Monolayers to Patterned Surfaces. *Prog. Polym. Sci.* **2012**, *37*, 157−181.
(36) Hui, C. M.; Pietrasik, J.; Schmitt, M.; Mahoney, C.; Choi, J.; Bockstaller, M. R.; Matyjaszewski, K. Surface-Initiated Polymerization as an Enabling Tool for Multifunctional (Nano-)Engineered Hybrid Materials. *Chem. Mater.* **2014**, *26*, 745−762.
(37) Balazs, A. C.; Singh, C.; Zhulina, E.; Chern, S.-S.; Lyatskaya, Y.; Pickett, G. Theory of Polymer Chains Tethered at Interfaces. *Prog. Surf. Sci.* **1997**, *55*, 181−269.
(38) Zhao, J.; Lai, H.; Lu, H.; Barner-Kowollik, C.; Stenzel, M. H.; Xiao, P. Fructose-Coated Nanodiamonds: Promising Platforms for Treatment of Human Breast Cancer. *Biomacromolecules* **2016**, *17*, 2946−2955.
(39) Zhan, N.; Palui, G.; Merkl, J. P.; Mattoussi, H. Bio-orthogonal Coupling as a Means of Quantifying the Ligand Density on Hydrophilic Quantum Dots. *J. Am. Chem. Soc.* **2016**, *138*, 3190−3201.
(40) Nebhani, L.; Barner-Kowollik, C. Orthogonal Transformations on Solid Substrates: Efficient Avenues to Surface Modification. *Adv. Mater.* **2009**, *21*, 3442−3468.
(41) Laradji, A. M.; McNitt, C. D.; Yadavalli, N. S.; Popik, V. V.; Minko, S. Robust, Solvent-Free, Catalyst-Free Click Chemistry for the Generation of Highly Stable Densely Grafted Poly(ethylene glycol) Polymer Brushes by the Grafting To Method and Their Properties. *Macromolecules* **2016**, *49*, 7625−7631.

DOI: 10.1021/acs.macromol.7b00286
Macromolecules 2017, 50, 3662−3670

(42) Papra, A.; Gadegaard, N.; Larsen, N. B. Characterization of Ultrathin Poly(ethylene glycol) Monolayers on Silicon Substrates. *Langmuir* **2001**, *17*, 1457−1460.
(43) Hensarling, R. M.; Doughty, V. A.; Chan, J. W.; Patton, D. L. "Clicking" Polymer Brushes with Thiol-yne Chemistry: Indoors and Out. *J. Am. Chem. Soc.* **2009**, *131*, 14673−14675.
(44) Theato, P.; Sumerlin, B. S.; O'Reilly, R. K.; Epps, T. H., III Stimuli Responsive Materials. *Chem. Soc. Rev.* **2013**, *42*, 7055−7056.
(45) Cao, Z.; Mi, L.; Mendiola, J.; Ella-Menye, J. R.; Zhang, L.; Xue, H.; Jiang, S. Reversibly Switching the Function of a Surface between Attacking and Defending against Bacteria. *Angew. Chem., Int. Ed.* **2012**, *51*, 2602−2605.
(46) Liu, D.; Xie, Y.; Shao, H.; Jiang, X. Using Azobenzene-Embedded Self-Assembled Monolayers to Photochemically Control Cell Adhesion Reversibly. *Angew. Chem., Int. Ed.* **2009**, *48*, 4406−4408.
(47) Desseaux, S.; Klok, H. A. Temperature-Controlled Masking/Unmasking of Cell-Adhesive Cues with Poly(ethylene glycol) Methacrylate Based Brushes. *Biomacromolecules* **2014**, *15*, 3859−3865.
(48) Zayas, H. A.; Lu, A.; Valade, D.; Amir, F.; Jia, Z.; O'Reilly, R. K.; Monteiro, M. J. Thermoresponsive Polymer-Supported-Proline Micelle Catalysts for the Direct Asymmetric Aldol Reaction in Water. *ACS Macro Lett.* **2013**, *2*, 327−331.
(49) Mastrotto, F.; Caliceti, P.; Amendola, V.; Bersani, S.; Magnusson, J. P.; Meneghetti, M.; Mantovani, G.; Alexander, C.; Salmaso, S. Polymer Control of Ligand Display on Gold Nanoparticles for Multimodal Switchable Cell Targeting. *Chem. Commun.* **2011**, *47*, 9846−9848.
(50) Won, S.; Richards, S.-J.; Walker, M.; Gibson, M. I. Externally Controllable Glycan Presentation on Nanoparticle Surfaces to Modulate Lectin Recognition. *Nanoscale Horiz.* **2017**, *2*, 106−109.
(51) Wu, C.; Wang, X. Globule-to-Coil Transition of a Single Homopolymer Chain in Solution. *Phys. Rev. Lett.* **1998**, *80*, 4092−4094.
(52) Li, Z.; Sun, L.; Zhang, Y.; Dove, A. P.; O'Reilly, R. K.; Chen, G. Shape Effect of Glyco-Nanoparticles on Macrophage Cellular Uptake and Immune Response. *ACS Macro Lett.* **2016**, *5*, 1059−1064.
(53) Patterson, J. P.; Robin, M. P.; Chassenieux, C.; Colombani, O.; O'Reilly, R. K. The Analysis of Solution Self-Assembled Polymeric Nanomaterials. *Chem. Soc. Rev.* **2014**, *43*, 2412−2425.
(54) Elsabahy, M.; Wooley, K. L. Design of Polymeric Nanoparticles for Biomedical Delivery Applications. *Chem. Soc. Rev.* **2012**, *41*, 2545−2561.
(55) Moughton, A. O.; Patterson, J. P.; O'Reilly, R. K. Reversible Morphological Switching of Nanostructures in Solution. *Chem. Commun.* **2011**, *47*, 355−357.
(56) Wei, K.; Su, L.; Chen, G.; Jiang, M. Does PNIPAM Block Really Retard the Micelle-to-Vesicle Transition of Its Copolymer? *Polymer* **2011**, *52*, 3647−3654.
(57) Blackman, L. D.; Wright, D. B.; Robin, M. P.; Gibson, M. I.; O'Reilly, R. K. Effect of Micellization on the Thermoresponsive Behavior of Polymeric Assemblies. *ACS Macro Lett.* **2015**, *4*, 1210−1214.
(58) Mabire, A. B.; Robin, M. P.; Quan, W. D.; Willcock, H.; Stavros, V. G.; O'Reilly, R. K. Aminomaleimide Fluorophores: A Simple Functional Group with Bright, Solvent Dependent Emission. *Chem. Commun.* **2015**, *51*, 9733−9736.
(59) Robin, M. P.; Wilson, P.; Mabire, A. B.; Kiviaho, J. K.; Raymond, J. E.; Haddleton, D. M.; O'Reilly, R. K. Conjugation-Induced Fluorescent Labeling of Proteins and Polymers Using Dithiomaleimides. *J. Am. Chem. Soc.* **2013**, *135*, 2875−2878.
(60) Robin, M. P.; Mabire, A. B.; Damborsky, J. C.; Thom, E. S.; Winzer-Serhan, U. H.; Raymond, J. E.; O'Reilly, R. K. New Functional Handle for Use as a Self-Reporting Contrast and Delivery Agent in Nanomedicine. *J. Am. Chem. Soc.* **2013**, *135*, 9518−9524.
(61) Robin, M. P.; O'Reilly, R. K. Strategies for Preparing Fluorescently Labelled Polymer Nanoparticles. *Polym. Int.* **2015**, *64*, 174−182.
(62) Robin, M. P.; Raymond, J. E.; O'Reilly, R. K. One-Pot Synthesis of Super-Bright Fluorescent Nanogel Contrast Agents Containing a Dithiomaleimide Fluorophore. *Mater. Horiz.* **2015**, *2*, 54−59.
(63) Mabire, A. B.; Brouard, Q.; Pitto-Barry, A.; Williams, R. J.; Willcock, H.; Kirby, N.; Chapman, E.; O'Reilly, R. K. CO_2/pH-Responsive Particles with Built-in Fluorescence Read-out. *Polym. Chem.* **2016**, *7*, 5943−5948.
(64) Cairo, C. W.; Gestwicki, J. E.; Kanai, M.; Kiessling, L. L. Control of Multivalent Interactions by Binding Epitope Density. *J. Am. Chem. Soc.* **2002**, *124*, 1615−1619.
(65) Lis, H.; Sharon, N. Lectins: Carbohydrate-Specific Proteins That Mediate Cellular Recognition. *Chem. Rev.* **1998**, *98*, 637−674.

DOI: 10.1021/acs.macromol.7b00286
Macromolecules 2017, 50, 3662−3670